

Digital FM Demodulator with Reduced Computational Complexity

Abstract. This paper describes a simple implementation of FM demodulator with reduced computational complexity. Key idea is to avoid sinus, cosine, arctan functions to increase performance at the expense of slightly reduced quality of demodulated signal. This allows implement the demodulator using simple microcontrollers without special digital signal processing features. Additional benefit is the possibility to demodulate FM signals in a relatively wide range, without changing of sampling and local oscillator frequencies.

Streszczenie. W artykule opisano prostą implementację demodulatora FM o zmniejszonej złożoności obliczeniowej. Kluczową ideą jest unikanie funkcji sinus, cosinus, arctan w celu zwiększenia wydajności kosztem nieco obniżonej jakości demodulowanego sygnału. Pozwala to na implementację demodulatora za pomocą prostych mikrokontrolerów bez specjalnych funkcji cyfrowego przetwarzania sygnału. Dodatkową korzyścią jest możliwość demodulacji sygnałów FM w stosunkowo szerokim zakresie, bez zmiany częstotliwości próbkowania i lokalnych oscylatorów. (Cyfrowy demodulator FM o zmniejszonej złożoności obliczeniowej).

Keywords: modulation, reduced complexity, digital demodulator.

Słowa kluczowe: modulacja, zredukowana złożoność, demodulator cyfrowy.

Introduction

The key idea of proposed in this paper FM demodulator [1-6] was to propose simple algorithm which avoids usage of sinus, cosine, arctan functions to be able implement it in simple microcontrollers which does not contain digital signal processing (DSP) hardware accelerators. The demodulator output signal could have not significant distortions in expense of applied few simplifications. Demodulation of the FM signals is widely used in various spheres of human activity, in particular, in the construction of interference-resistant information transmission systems and microwave motion sensors with modulation of the electromagnetic oscillations reflected back from the explored object [7, 8].

Basis of considered in this paper FM demodulator is approach used in polar frequency discriminator. Typical structure of polar frequency discriminator is shown in Figure 1.

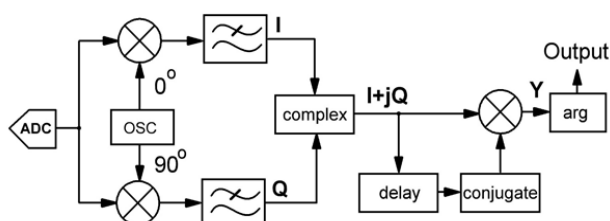


Fig.1. Typical structure of polar FM discriminator

The input analog FM signal is digitized using analog-to-digital converter (ADC) [9]. Then the in-phase (I) and quadrature (Q) components are obtained by multiplying by the local oscillator frequency and applying of the low pass filters (LPF). Then I and Q are considered as complex numbers and polar discrimination is performed by multiplication of current complex sample by delayed and conjugated complex sample. The product of such multiplication is denoted as Y . And finally, the argument of product Y is calculated, usually using arctan function, which is the FM demodulator output signal and corresponds to modulating signal.

Mathematical Justifications of Considered Simplifications

The main purpose of this chapter is to show that at specific value of delay in the polar frequency discriminator the approximate value of modulating signal could be obtained by calculating only the imaginary part of product Y in Figure 1.

The FM-signal in general is described by the following equation:

$$(1) \quad s(t) = A_c \cdot \sin(2\pi f_c t + \varphi_{FM}(t) + \varphi_0)$$

where: A_c – amplitude of carrier, f_c – frequency of carrier, φ_0 – initial phase of carrier, φ_{FM} – phase shift caused by frequency modulation.

Let consider φ_0 equal to zero for simplification as it does not impact to the final results.

The equations describing time dependencies I and Q components are the following:

$$(2) \quad \begin{aligned} I(t) &= A_c \cdot \sin(2\pi f_c t + \varphi_{FM}(t)) \cdot A_{osc} \cdot \sin(2\pi f_{osc} t) = \\ &= \frac{A_c \cdot A_{osc}}{2} \cdot (\cos(2\pi f_c t + \varphi_{FM}(t) - 2\pi f_{osc} t)) - \\ &- \frac{A_c \cdot A_{osc}}{2} \cdot (\cos(2\pi f_c t + \varphi_{FM}(t) + 2\pi f_{osc} t)) \end{aligned}$$

$$(3) \quad \begin{aligned} Q(t) &= A_c \cdot \sin(2\pi f_c t + \varphi_{FM}(t)) \cdot A_{osc} \cdot \cos(2\pi f_{osc} t) = \\ &= \frac{A_c \cdot A_{osc}}{2} \cdot (\sin(2\pi f_c t + \varphi_{FM}(t) - 2\pi f_{osc} t)) + \\ &+ \frac{A_c \cdot A_{osc}}{2} \cdot (\sin(2\pi f_c t + \varphi_{FM}(t) + 2\pi f_{osc} t)) \end{aligned}$$

where: A_{osc} – amplitude of local oscillator, f_{osc} – frequency of local oscillator.

After simplification and considering that LPF filter suppresses frequency component ($f_c + f_{osc}$) the equations for I and Q components will look as below:

$$(4) \quad I(t) = \frac{A_c \cdot A_{osc}}{2} \cdot \cos(2\pi(f_c - f_{osc})t + \varphi_{FM}(t))$$

$$(5) \quad I(t) = \frac{A_c \cdot A_{osc}}{2} \cdot \sin(2\pi(f_c - f_{osc})t + \varphi_{FM}(t))$$

Per structure shown in Figure 1 the output of polar discriminator is a complex number obtained by multiplication of current complex sample and delayed conjugated complex sample. Let denote current complex sample as $I + jQ$ and delayed conjugated sample as $I' - jQ'$ and express the result of their multiplication Y :

$$(6) \quad Y = (I + jQ) \cdot (I' - jQ') = I \cdot I' + Q \cdot Q' + j(Q \cdot I' - I \cdot Q')$$

The output signal in Figure 1 is obtained as argument of Y which could be calculated as arctan of relation of imaginary to the real part of Y . Considering small angle approximation, the output signal of demodulator could be expressed as follow:

$$(7) \quad S_{out} = \arg(Y) = \arctan\left(\frac{Im(Y)}{Re(Y)}\right) \approx Im(Y)$$

at small $Im(Y)$.

In Equations (4) and (5) let denote $\frac{A_c \cdot A_{osc}}{2}$ as A .

Considering Equations (4), (5) and (7), the output signal could be expressed as below:

$$(8) \quad \begin{aligned} S_{out} &\approx Im(Y) = Q \cdot I' - I \cdot Q' = \\ &= A^2 \cdot \sin(2\pi(f_c - f_{osc}) \cdot t + \varphi_{FM}(t)) \times \\ &\times \cos(2\pi(f_c - f_{osc}) \cdot (t - \Delta t) + \varphi_{FM}(t - \Delta t)) - A^2 \times \\ &\times \cos(2\pi(f_c - f_{osc}) \cdot t + \varphi_{FM}(t)) \times \\ &\times \sin(2\pi(f_c - f_{osc}) \cdot (t - \Delta t) + \varphi_{FM}(t - \Delta t)) \end{aligned}$$

This expression could be considered as:

$$(9) \quad Im(Y) = A^2 \cdot (\sin(\alpha) \cdot \cos(\beta) - \cos(\alpha) \cdot \sin(\beta))$$

where: $\alpha = 2\pi(f_c - f_{osc}) \cdot t + \varphi_{FM}(t)$ and $\beta = 2\pi(f_c - f_{osc}) \cdot (t - \Delta t) + \varphi_{FM}(t - \Delta t)$.

By applying the angle difference trigonometrical identity to the expressions above the $Im(Y)$ could be expressed as:

$$(10) \quad \begin{aligned} Im(Y) &= A^2 \cdot \sin(\alpha - \beta) = A^2 \times \\ &\times \sin(2\pi(f_c - f_{osc}) \cdot \Delta t + \varphi_{FM}(t) - \varphi_{FM}(t - \Delta t)) \end{aligned}$$

In the expression above it could be proven that at specific values of Δt (delay in polar discriminator), the $Im(Y)$ is zero in case of no FM modulation ($\varphi_{FM}(t) - \varphi_{FM}(t - \Delta t) = 0$). This specific delay could be obtained from the following equation:

$$(11) \quad n \cdot \pi = 2\pi(f_c - f_{osc}) \cdot \Delta t, \text{ where } n \in Z$$

By solving this equation, the delay is calculated by the following expression:

$$(12) \quad \Delta t = \frac{n}{2 \cdot |f_c - f_{osc}|}$$

This delay physically is the number of beat half periods caused by difference of carrier and local oscillator frequencies.

In case of FM modulation is present and value of Δt fulfills the expression above the $Im(Y)$ is calculated as below:

$$(13) \quad Im(Y) = A^2 \cdot \sin(\varphi_{FM}(t) - \varphi_{FM}(t - \Delta t))$$

And considering small angle approximation the output signal is calculated with the following expression:

$$(14) \quad S_{out} \approx A^2 \cdot (\varphi_{FM}(t) - \varphi_{FM}(t - \Delta t))$$

Note, in equation (14) it is considered that phase shift $\varphi_{FM}(t) - \varphi_{FM}(t - \Delta t)$ caused by modulating signal is small enough that allows applying the small angle approximation. This expression shows that output signal is proportional to the phase shift caused by modulating signal and correspondingly to modulating signals itself.

In general, the phase caused by FM modulation is defined by the following expression:

$$(15) \quad \varphi_{FM}(t) = K_f \cdot \int_0^t S_m(t) dt$$

where: K_f – frequency sensitivity, $S_m(t)$ – modulating signal.

The phase shift caused by modulating signal during delay Δt is defined by the following expression:

$$(16) \quad \varphi_{FM}(t) - \varphi_{FM}(t - \Delta t) = K_f \cdot \int_{t-\Delta t}^t S_m(t) dt$$

Digital Form

This chapter devoted to provide important expressions in case of digital implementation of FM demodulator. Let consider that all processing is performed in digital form and input FM signal is sampled at frequency f_s . Considering Equation (12) the delay of polar discriminator, represented in samples count, is calculated as follow:

$$(17) \quad \text{delay} = \text{round}\left(\frac{f_s \cdot n}{2 \cdot |f_c - f_{osc}|}\right)$$

where: *round* – operation of rounding number to the nearest integer, f_s – sampling frequency.

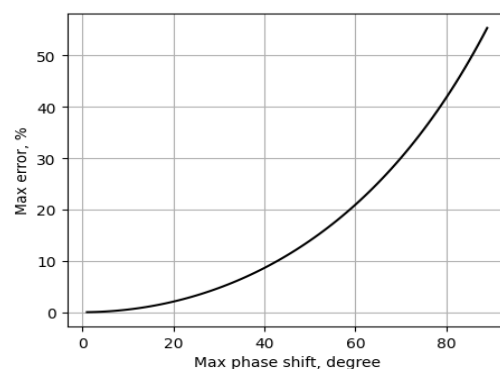


Fig.2. The instant error caused by small angle approximation versus phase shift

The maximal phase shift caused by modulating signal considering Equation (16) in the worst case when modulating signal $S_m(t)$ is stable at its maximal value equal to the amplitude of modulating signal A_m is calculated as follow:

$$(18) \quad Shift_{\varphi} = \frac{K_f \cdot A_m \cdot delay}{f_s}$$

The worst instant error caused by small angle approximation versus phase shift, calculated by Equation (18), is shown in Figure 2.

Simplified Digital FM Demodulator

In this chapter the structure of proposed FM demodulator is described with several peculiarities which were explained above using mathematical justification. The simplified version of FM demodulator is shown in Figure 3.

The first simplification is that local oscillator uses the square orthogonal functions instead of sinus and cosine functions. The orthogonal functions could take values of 1 or -1 only. From the implementation point of view, it means do not change the input sample in case of "1" and just invert its sign in case of "-1". Then the resulting samples are feed to the LPFs. To implement delay of *I* and *Q* components two circular buffers are used with size corresponds to required delay.

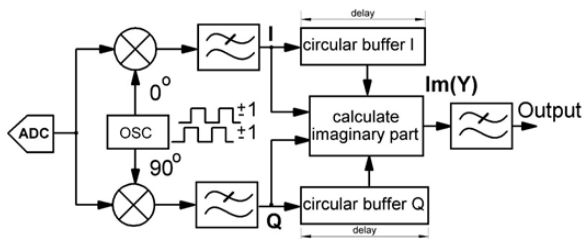


Fig.3. Simplified version of FM demodulator

The second simplification is that small-angle approximations is applied at step of arctan calculation. It means that such delay of complex sample is used at which imaginary part of complex number is approximately equal to its argument. So, in Figure 3 the only imaginary part of complex number obtained as product *Y* in Figure 1 is calculated. The result is passed to the LPF which optionally could be used to reduce high frequency component caused by rounding of *delay* calculated by Equation (17).

The relation of sampling frequency to local oscillator frequency f_{osc} must be multiple of 4 as shown below:

$$(19) \quad f_s = 4 \cdot oversampling \cdot f_{osc}, \quad oversampling \in \mathbb{Z}_+$$

For example, in case of $oversampling = 1$ the local oscillator in Figure 3 produces the following sequences:

$$(20) \quad I_{osc} = [1, 1, -1, -1]; \quad Q_{osc} = [1, -1, -1, 1]$$

in case of $oversampling = 2$ the following:

$$(21) \quad I_{osc} = [1, 1, 1, 1, -1, -1, -1, -1]; \\ Q_{osc} = [1, 1, -1, -1, -1, -1, 1, 1]$$

and so on.

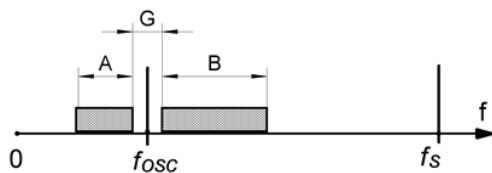


Fig.4. Illustration of frequency ranges: A and B – ranges where FM signal could be demodulated without changes of sampling f_s and local oscillator frequencies f_{osc} , G – gap between ranges where FM signals could not be demodulated

Figure 4 shows peculiarities of considered FM demodulator in terms of frequency ranges where FM signal could be demodulated.

There are two ranges A and B where the FM signal could be demodulated without changes of sampling and local oscillator frequencies. Between these ranges there is a gap G where FM signals could not be demodulated. The center of this gap is local oscillator frequency. The width of this gap is relatively very small in comparison with ranges A and B and is explained in chapters above. But in case of FM signal located in this gap G the only way is to change sampling or local oscillator frequency.

Low Pass Filters Consideration

For the most of configurations of proposed FM demodulator the 1-st order IIR LPF filter could be used with the following parameters: passband up to 0,1 of sampling frequency with nonuniformity -6 dB, stopband starting from 0,35 of sampling frequency with -20 dB attenuation. The structure and amplitude frequency response of such digital filter is shown in Figure 5.

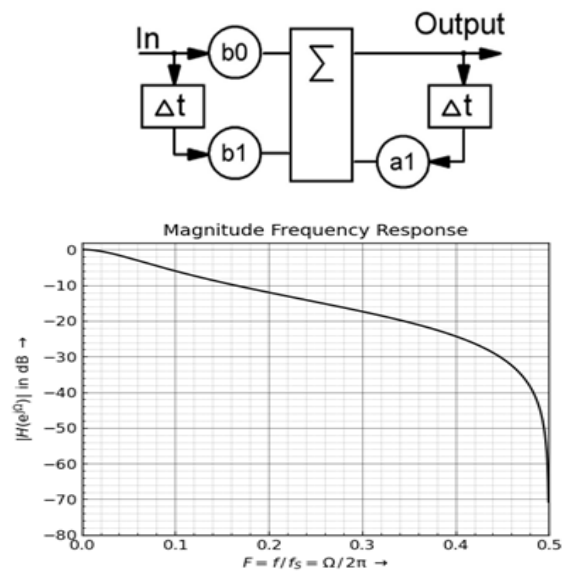


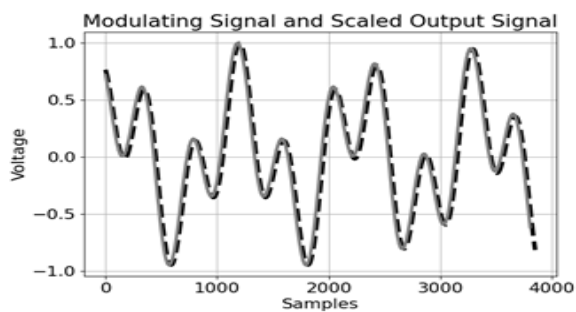
Fig.5. The first order IIR filter (a) and its frequency response (b) used in proposed FM demodulator

The coefficients $b_0 = b_1 = 0,1584$ and $a_1 = -0,6832$ were obtained using Filter Design Analysis tool PyFDA. Alternative filters could be applied depending on computation capabilities.

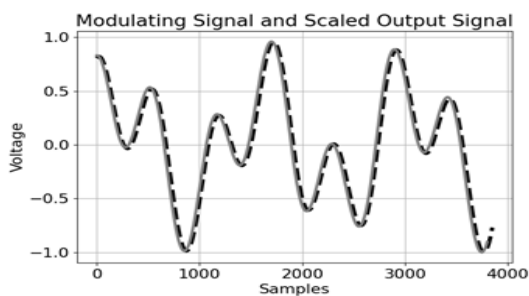
Verification with Python Model

The Python verification model could be found at the following GitHub repository: <https://github.com/mspartak/science> in folder "demodulator_nfm".

File demodulator_nfm.py contains Python class which implements proposed in this paper FM demodulator. After instantiation of the object of this class the method <init> need to be called. Then each sample of FM signal need to be processed by <demodulate_nfm> method which return one sample of demodulated signal. The <demodulate_nfm> function could be easily adapted to microcontrollers implementation, for example using C language. The usage example is in the testbench Python script in file <demodulator_testbench.py>. The script <demodulator_model.py> contains the same model organized in more readable way, but not applicable for direct implementation in microcontrollers, because it uses Python libraries functions.

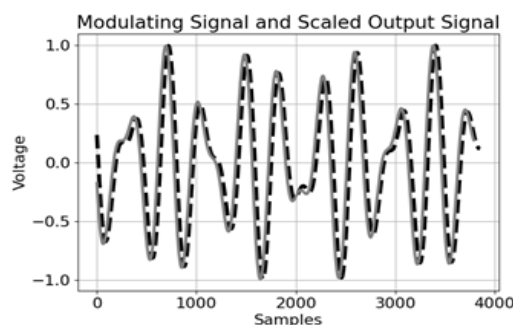


$f_c = 108,9$ kHz;
modulating signal: 370 Hz @ 0,5 V + 962 Hz @ 0,5 V;
delay 46 samples (2 beat half periods)

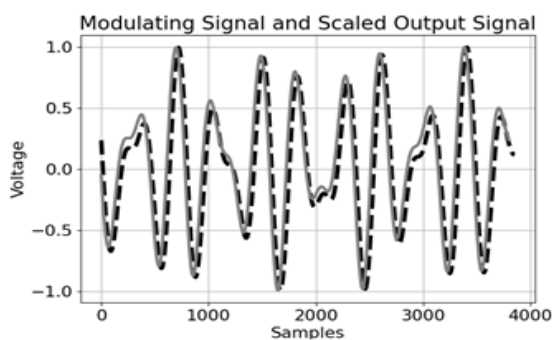


$f_c = 104,0$ kHz;
modulating signal: 280 Hz @ 0,5 V + 690 Hz @ 0,5 V;
delay 50 samples (1 beat half period)

Fig.6. The scaled output signal (gray curve) and modulating signal (black dashed curve)



$f_c = 103,2$ kHz; delay 62 samples
(1 beat half period)



$f_c = 154,3$ kHz; delay 52 samples
(14 beat half periods)

Fig.7. The scaled output signal (gray curve) and modulating signal (black dashed curve) obtained for carrier frequency close (top) and far (bottom) to the local oscillator frequency. Modulating signal: 1040 Hz @ 0,6 V + 1490 Hz @ 0,4 V

Figure 6 shows two examples of the output signal obtained using Python model. The gray solid curves show the linearly scaled demodulator output signal and the black dashed curves show the modulating signals. Linear scaling

is applied to show it on the same plot with the modulating signal and to show that output signal waveform matches to the modulating signal pretty well.

Figure 7 shows example how the same modulating signal is applied to different carrier frequencies. In Figure 7 (left) the carrier frequency is relatively close to the local oscillator frequency and in Figure 7 (right) it is far, but as it is shown the waveforms in both cases match to the modulating signal pretty well. Additionally, it is visible that signal is inverted in Figure 7. It is due to the number of beat half periods n in Equation (17) is odd in left plot and even in right plot.

The other parameters used in these examples are as follow: $oversampling = 1$; $K_f = 1000$ Hz/V; carrier amplitude $A_c = 1$ V. Modulating signal described as sum of harmonics with given frequencies and amplitudes. For instance, modulating signal 370 Hz @ 0,5 V + 962 Hz @ 0,5 V means that it obtained as sum of two harmonics with frequencies 370 Hz and 962 Hz and amplitude 0,5 V each of them.

Some more examples are in the GitHub link mentioned above in subfolder "results". Also, the custom examples could be obtained by changing the input parameters in the <demodulator_testbench.py> script and executing it.

Conclusions

This paper describes a simple implementation of FM demodulator. The strict recommendations and tuning explained in this paper need to be considered in order to obtain proper work of the demodulator.

As it is shown in Equations (17) and (18) the following conclusions could be made and considered during the implementation:

1) Increasing of *delay* increases $Shift_\phi$ causing to increasing of error. At the same time the sensitivity of demodulator to phase shift caused by FM modulation is increased per Equation (14);

2) The output signal is inverted if *delay* consist of odd number of half beat periods comparing to signal when *delay* consists of even number of half beat periods as was shown in Figure 7;

3) At small value of $|f_c - f_{osc}|$ per Equation (17) the value of *delay* increased and leads to large value of $Shift_\phi$. So, cases $f_c = f_{osc}$ and $f_c \approx f_{osc}$ caused to not possible usage of demodulator when carrier frequency is close to the local oscillator frequency;

4) For the particular value of $|f_c - f_{osc}|$ and parameters of FM signal the parameters *delay* need to be calculated and the $Shift_\phi$ evaluated. Such tuning of FM demodulator needs to be done to tune to the necessary carrier frequency;

5) The *delay* calculated by Equation (17) involves rounding to the nearest integer. This causes to appearance of high frequency component on the demodulator output. But usage of LPF filter on its output suppresses this component good enough.

Advantages of considered in this paper FM demodulator:

- Fully avoided sinus, cosine and arctan functions that allow to increase the performance at the expense of slightly reduced quality of demodulated signal caused by small angle approximation. Approximately the following computation needed to be done for each sample of FM signal: 10 to 13 multiplications, 9 additions, few assignments and logical operations;

- The local oscillator don't need to be precisely tuned to carrier frequency, but instead the parameter *delay* needs to be recalculated. The FM signal could be demodulated in relatively wide range of carrier frequencies;
- Python model is available to tune and verify FM demodulator with variety of parameters.

The drawback of considered in this paper FM demodulator is the not significant distortion of the output signal due to application of a small angle approximation. This could lead to limitation of wideband FM signals demodulation.

Authors: *sen. lect., PhD Spartak Mankovskyy, Lviv Polytechnic National University, Institute of Telecommunications, Radioelectronics and Electronic Engineering, Department of Radioelectronic Devices and Systems, Profesorska Str. 2, 79000, Lviv, Ukraine, E-mail: spartak.v.mankovskyy@lpnu.ua; assoc. prof., PhD Yuriy Matiieshyn, Lviv Polytechnic National University, Institute of Telecommunications, Radioelectronics and Electronic Engineering, Department of Radioelectronic Devices and Systems, Profesorska Str. 2, 79000, Lviv, Ukraine, E-mail: yurii.m.matiieshyn@lpnu.ua.*

REFERENCES

- [1] Yu F., Digital Demodulator for Frequency Modulated Signals, *Master's thesis*, Nanyang Technological University, 2005. Available at: https://dr.ntu.edu.sg/bitstream/10356/2566/1/SCE-THESES_308.pdf [Accessed: 12.03.2023].
- [2] Shima J.M., FM Demodulation Using a Digital Radio and Digital Signal Processing, *Master's thesis*, University of Florida, 1995. Available at: <https://www-elec.inaoep.mx/~rogerio/Digradio.pdf> [Accessed: 12.03.2023].
- [3] Xue R., Xu Q., Chang K. F., Tam K. W., A new method of an IF I/Q demodulator for narrowband signals, *IEEE International Symposium on Circuits and Systems*, Kobe, Japan, 2005, 3817-3820. Available at: <https://doi.org/10.1109/ISCAS.2005.1465462> [Accessed: 12.03.2023].
- [4] Song Bang-Sup, Lee In Seop, A digital FM demodulator for FM, TV, and wireless, *IEEE Transactions on Circuits and Systems II: Analog and Digital Signal Processing*, 42 (1995), No. 12, 821-825. Available at: <https://doi.org/10.1109/82.476180> [Accessed: 12.03.2023].
- [5] Punalchard R., Koseeyaporn J., Wardkein P., Novel digital FM Demodulation, *TENCON - IEEE Region 10 Conference*, Singapore, 2009, 1-4. Available at: <https://doi.org/10.1109/TENCON.2009.5395789> [Accessed: 12.03.2023].
- [6] Kuzyk A., Prudyus I., Sumyk M., Research of the discrete frequency-modulated signals properties, *International Conference on Modern Problem of Radio Engineering, Telecommunications and Computer Science*, Lviv, Ukraine, 2012, 103-103. Available at: <https://ieeexplore.ieee.org/document/6192414> [Accessed: 12.03.2023].
- [7] Miskiv A., Miskiv V.-M., Prudyus I., Yankevych R., Fabirovskyy S., Model of the Periodic Autocorrelation Function of Code Binary Sequences for Wireless Noise Immune Data Transmission Systems Signals Synthesis, *IEEE 4th International Symposium on Wireless Systems within the International Conferences on Intelligent Data Acquisition and Advanced Computing Systems*, Lviv, Ukraine, 2018, 221-224. Available at: <https://doi.org/10.1109/IDAACS-SWS.2018.8525523> [Accessed: 12.03.2023].
- [8] Prudyus I. N., Storozh V. G., Naida N.-V. I., Forming the sensitive area of microwave motion sensor, *XI International Conference on Antenna Theory and Techniques*, Kyiv, Ukraine, 2017, 291-293. Available at: <https://doi.org/10.1109/ICATT.2017.7972646> [Accessed: 12.03.2023].
- [9] Mankovskyy S., Nykolyshyn M., Mankovska E. Digital Method of SSB Modulation, *Computational Problems of Electrical Engineering*, 7 (2017), No. 2, 92-96. Available at: <https://science.lpnu.ua/sites/default/files/journal-paper/2018/sep/14625/5.pdf> [Accessed: 12.03.2023].